Kovove Mater. 48 2010 87–95
DOI: 10.4149/km_2010_2_87

Mechanical properties of particle reinforced titanium and titanium alloys

C. Poletti[1]*, G. Höltl[1,2]

[1] *Institute of Materials Science and Technology, Vienna University of Technology, Karlsplatz 13/E308, A-1040 Vienna, Austria*
[2] *Present address: Leobersdorfer Maschinenfabrik, GmbH & Co. KG, Südbahnstraße 28, A-2544 Leobersdorf, Austria*

Received 30 July 2009, received in revised form 8 October 2009, accepted 7 December 2009

Abstract

Titanium grade 2, Ti-6Al-4V and Ti-6Al-6V-2Sn unreinforced and reinforced with 10–15 vol.% SiC particles, 5 vol.% TiB whiskers and 12–20 vol.% TiC are characterized by compression tests, micro-, macro- and nano-hardness measurements, and X-ray diffraction. The measured Young's moduli up to 350 °C were found to be described using the Halpin Tsai model for the TiC and of TiB reinforced materials (aspect ratio of 1 and 100, respectively). The strengthening by SiC addition is attributed to matrix strain hardening due to the thermal misfit between the matrix and the reinforcement. The strengthening of TiC reinforced material is attributed to interstitial C dissolved in the alpha phase proved with the nanohardness results. TiB precipitates produce strengthening by grain refinement and dispersion hardening. The presence of 1 wt.% of C in the matrix also should be the reason for higher Young's modulus and strengthening.

K e y w o r d s: metal-matrix composites (MMCs), mechanical properties, deformation, elastic properties, powder metallurgy

1. Introduction

Titanium alloys show high specific mechanical properties up to high temperatures and good corrosion resistance. Therefore, they are attractive not only for aerospace components, but also for demanding automotive, process and medical applications [1]. Ceramic reinforcement can further improve some mechanical properties [2, 3]. Regarding metal matrix composites (MMC), particulate reinforced alloys (PRM) are cheaper than the continuous fibre reinforced alloys, and can be forged, cut, formed, and their properties are more or less isotropic. Deformation maps show the limits of hot working of composites compared to their matrices [4].

The reinforcements investigated in previous works are carbides: TiC [5], SiC [6, 7]; nitrides: TiN [8], Si_3N_4 [2]; borides: TiB_2, TiB [9, 10]; oxides: Al_3O_2 (in titanium aluminides [11]), TiO_2 [12], Zr_2O_3, RE_2O_3 (with RE = rare earth element) [13]; or intermetallic compounds: Ti_5Si_3 [14]. Table 1 shows some properties of these reinforcements. Stiffness increment and strengthening of PRM depend on the volume fraction, size distribution and chemical stability of the reinforcing phase. Some aspects related to reinforcement nature, shape and distribution are discussed in this work.

1.1. Elastic behaviour

In general, higher Young's modulus of the reinforcement E_F with respect to E_M of the matrix is exploited for metal matrix composites to increase the specific stiffness. The semi-empirical approximation developed by Halpin and Tsai [15] for the Young's modulus E_C for particle reinforced materials is calculated by:

$$E_C = E_M\,(1 + \xi\eta f)\,/\,(1 - \eta f)\,,$$
$$\eta = \left(\frac{E_F}{E_M} - 1\right) \Big/ \left(\frac{E_F}{E_M} + \xi\right), \qquad (1)$$

*Corresponding author: tel.: +43-1-5880130818; fax: +43-1-5880130899; e-mail address: cpoletti@mail.zserv.tuwien.ac.at

Table 1. Relevant properties of components of Ti matrix composites

	Young's modulus (GPa)	Linear coefficient of thermal expansion (10^{-6} K^{-1}) < 300 °C	Stability at processing temperature
Ti64	115	8.8	β-transus 1000 °C
TiB	550	8.6	very stable
TiC	460	7.4	stable
TiN	250	9.3	
SiC	420	4.3	forming TiC_x, Ti_5Si_3 and $Ti_5Si_3C_x$
Si_3N_4	320	3.2	forming Ti_5Si_3 and Ti_3Si
TiB_2	529	6.4	forming TiB from Ti + TiB_2
B_4C	449	4.5	forming TiC and TiB
Al_2O_3	350	8.1	forming $TiAl_3$ and TiO

where ξ is an empirical parameter that depends mainly on processing factors (for high quality discontinuously reinforced metals in the order of 1), η is the reinforcement efficiency factor (depending on the orientation of elongated reinforcements) and f its volume fraction.

For randomly distributed short fibres, the Young's modulus can be calculated as:

$$E_{\text{random}} = \frac{3}{8}E_{11} + \frac{5}{8}E_{22},$$
$$E_{11} = \frac{1 + 2\,(l_{\text{f}}/d_{\text{f}})\,\eta_{\text{L}} f}{1 - \eta_{\text{L}} f}E_{\text{m}},$$
$$E_{22} = \frac{1 + 2\eta_{\text{T}} f}{1 - \eta_{\text{T}} f}E_{\text{m}}, \tag{2}$$

where the reinforcement efficiency factors in the direction (L) η_{L} and transversal (T) to the fibre direction η_{T} are given by:

$$\eta_{\text{L}} = \left(\frac{E_{\text{f}}}{E_{\text{M}}} - 1\right) \Big/ \left(\frac{E_{\text{f}}}{E_{\text{M}}} + 2\frac{l_{\text{f}}}{d_{\text{f}}}\right),$$
$$\eta_{\text{T}} = \left(\frac{E_{\text{f}}}{E_{\text{M}}} - 1\right) \Big/ \left(\frac{E_{\text{f}}}{E_{\text{M}}} + 2\right), \tag{3}$$

where l_{f} is the average length and d_{f} the diameter of the fibres.

1.2. Strengthening

Since fabrication of MMCs involves consolidation at relatively high temperatures, mismatch stresses are created during cooling to ambient temperatures. If T_{esf} is a temperature in an effectively stress-free state, then the linear misfit strain is simply $\Delta\alpha\Delta T$, where $\Delta T = T_{\text{esf}} - T_{\text{ambient}}$ and the mismatch in the coefficient of linear thermal expansion (α) $\Delta\alpha = \alpha_{\text{M}} - \alpha_{\text{F}}$. The corresponding elastic stress is limited by the yield strength of the matrix. The distribution of the stress produced by local plastic flow can limit the hoop or tangential tensile stress near the particle.

The reinforcement brings also changes in the microstructure of the matrix provoked by:

– *Dislocation strengthening.* The dislocation density increases either as a result of applied straining or by the thermally induced stresses derived from $\Delta\alpha$. Miller and Humphreys [16] predict the dislocation density increment ($\Delta\rho$) by:

$$\Delta\rho = 12\frac{\Delta\alpha\Delta T f}{bd}, \tag{4}$$

where b is the Burgers vector and d the particle diameter. The influence of dislocation density on the variation of the matrix strength $\Delta\sigma_{\text{YM}}$ is:

$$\Delta\sigma_{\text{YM}} \propto Gb\sqrt{\rho}. \tag{5}$$

– *Strengthening due to grain refinement.* The contribution to the yield strength of the grain refinement can be estimated using the Hall-Petch relation:

$$\Delta\sigma_{\text{YM}} \approx \beta D^{-1/2}, \tag{6}$$

where β is typically 0.1 MPa m$^{1/2}$ and D is the grain size.

1.3. Chemical stability

Chemical reactions between matrix and reinforcement can occur at high temperatures during consolidation of the composite. The reaction between SiC and Ti produces brittle silicides [17], decreasing the performance of the composite. This was avoided by short exposure times at high temperatures during its production [4]. TiB_2 is converted into TiB as long as the average B concentration in the reaction zone is less than 18–18.5 wt.% [18]. TiC is the most stable carbide, but some investigations showed that at high temperatures C diffuses into the titanium matrix, retained as interstitial element [19].

Table 2. Investigated materials and processing methods

Matrix	Reinforcement	Production	Producer	Name
Ti grade 2	0 %	Ingot, cogged.		Ti G2
	SiC 15 vol.%	PM, hot pressing at 950 °C	ARCS	Ti/SiC/10p (HP)
	SiC 8 vol.%	PM, hot extrusion at 850 and 900 °C	TU Vienna	Ti/SiC/15p (HE)
Ti64	0 %	Ingot, cogged		Ti64 Ingot
	TiB 5 vol. %	PM, CHIPing (*in situ*)	Crucible	Ti64/TiB/5w
Ti662	0 %	PM, CHIPing at RT and 1000 °C	Dynamet	Ti662 PM
	TiC 12 vol.%	PM, CHIPing at RT and 1000 °C	Dynamet	Ti662/TiC/12p
	TiC 20 vol.%	PM, CHIPing at RT and 1000 °C	Dynamet	Ti662/TiC/20p

ARCS – Austrian Research Center, Seibersdorf, Austria
TU Vienna – Institute of Chemical Technologies and Analytics, Vienna University of Technology, Austria
Dynamet – Dynamet Technology, Inc.
Crucible – Crucible Research; Crucible Materials Corporation

2. Experimental

Ti based composites and matrices described in Table 2 were tested. The composite reinforced with TiC was produced by mixing the TiC particles with the pre-alloyed titanium matrix powders before densification by cold isostatic pressing, sintering at around 1100 °C followed by hot isostatic pressing at the same temperature (CHIPing). The matrix sample of Ti-6Al-6V-2Sn (Ti662) was produced in the same way.

The Ti64/TiB/5w was produced by melting Ti pre alloyed with 6 wt.% Al and 4 wt.% V, with 1 wt.% of B and 0.1 wt.% of C powder, and the same CHIPing procedure as before explained was applied. During CHIPing around 5 vol.% TiB whiskers precipitate *in situ.*

Pure Ti was reinforced with SiC particles by powder hot extrusion at 900 °C. The production and microstructural features of the materials reinforced with SiC are described in [7].

Ti grade 2 and Ti-6Al-4V (Ti64) ingot materials were produced using the commercial route to obtain equiaxed grains; the processes include alpha-beta thermo-mechanical treatments. The compression samples taken from the ingot materials were machined to orient the compression axis parallel to the cogging direction.

The microstructure of the samples was studied by scanning electron microscope (SEM), field emission gun (FEG)-SEM and by light optical microscopy (LOM) after etching 15 s with a Kroll solution. Axio Vision Software was used to quantify the vol.% and shape factor of the reinforcements. The grain size of Ti grade 2 and SiC reinforced Ti was estimated using the interception ASTM E112 method.

The compression tests of cylindrical specimens were carried out in a Gleeble®1500 machine at 350 °C and in a ZWICK universal tests machine at room temperature and at 0.005 s^{-1} of strain rate. In the Gleeble®1500, the samples were heated at 10 K s^{-1} up to 350 °C and held at this temperature for 30 s before deformation.

Micro- and macrohardness measurements were carried out at RT using the $HV_{0.05-0.1}$ and HV_1 methods, respectively. Microhardness of the matrix was measured without touching any ceramic particle observed at the surface. In the case of Ti64/TiB/5w only the big TiB needles could be avoided. Nanohardness was measured at RT to determine the hardness of alpha and beta phases of unreinforced and reinforced Ti662.

Dynamical mechanical analysis (DMA) was used to determine the Young's modulus from RT to 350 °C, using the DMA 2980 (TA Instruments) device in the 3 point bending mode. Specimens of 55 × 4 × 2 mm^3 were heated at 3 K min^{-1}, and strained to amplitude of 40 μm at a frequency of 1 Hz.

X-ray diffractometry was carried out with a Co-tube on polished samples to identify the phases in the TiC and TiB reinforced materials.

3. Results

3.1. Microstructure and phases

Figure 1 shows the microstructure of the unreinforced matrices. Ti grade 2 is formed by equiaxed alpha grains (Fig. 1a). The grain size was estimated to be 60 μm. In Fig. 1b, Ti662 PM shows lamella alpha colonies surrounded by relatively big alpha along the prior beta grain. Between the alpha phases, beta field is observed. Ti64 ingot shows bimodal microstructure (Fig. 1c) with elongated alpha grains in the longitudinal direction and fine acicular alpha phase embedded in the beta phase.

Figure 2 shows the as received microstructures of the titanium based composites tested in this work. In Figs. 2a–c, Ti64 reinforced with TiB shows a matrix

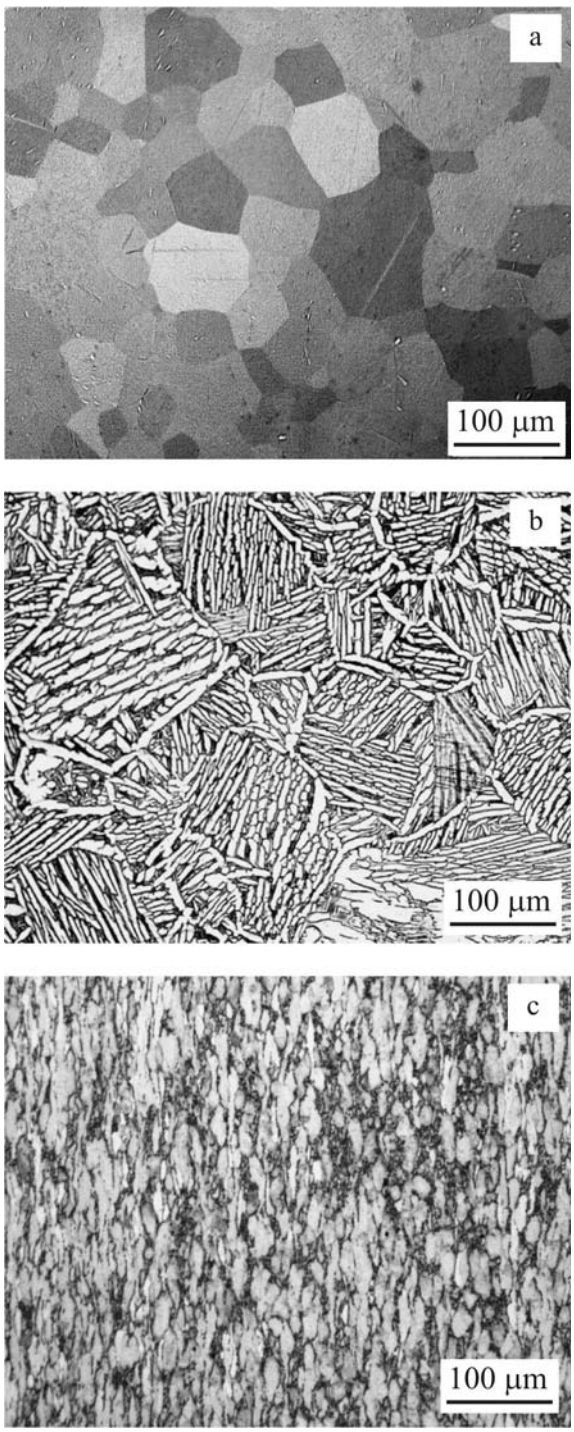

Fig. 1. SEM micrographs showing a) equiaxed alpha grains in titanium grade 2, b) lamellar alpha colonies (white) with beta phase in between (grey) in PM Ti662, c) alpha-grains (bright) elongated in the cogging direction (Ti64).

with fine alpha grains, and two types of TiB precipitates in concordance with [20]:

– Small TiB precipitates formed from the reaction $Ti + B \rightarrow TiB_2$ followed by the reaction $TiB_2 + Ti \rightarrow 2TiB$ provoked by the excess of titanium. The mean cross section of these particles is around 0.4 µm^2 and the ratio $feret_{max}/feret_{min}$ of about 10 (Fig. 2c).

– Clusters of large TiB needles surrounded by small TiB needles (Fig. 2b). The mean area of these particles is around 10 µm^2, and the $feret_{max}/feret_{min}$ is about 5.

Figures 2d,e show Ti662 reinforced with TiC. The microstructure consists of smaller alpha grains than the unreinforced PM material, and an inhomogeneous distribution of the reinforcement concentrated along the original Ti-alloy powder grain boundaries. Little porosity was observed within particle clusters. The mean particle size is 10 µm and the mean shape factor = 0.6 (elongated particles).

Ti with SiC particles neither shows reaction zones nor porosity (Figs. 2f,g). The α Ti grains are finer (20 µm) than in unreinforced Ti grade 2.

X-ray measurements on Ti64/TiB/5w only show peaks of orthorhombic TiB. TiC reinforced titanium alloy exhibits only TiC and titanium matrix. Ti_2C [21] was not revealed in the diffraction pattern. The lattice parameters of the phases in the Ti662 sample and the TiC reinforced material are (in Å):

– Alpha phase: $a = 2.925251(6)$ and $c = 4.67560(1)$ for Ti662 and $a = 2.92544(1)$ and $c = 4.67944(2)$ for Ti662/TiC/12p.

– Beta phase: $a = 3.214434(9)$ for Ti662 and $a = 3.22056(2)$ for Ti662/TiC/12p.

– TiC: $a = 4.30334$. The value is smaller than in [22].

The alpha and beta phases are bigger in the composite than in the unreinforced material, probably due to interstitial C. The smaller lattice parameter value of TiC compared to the literature value presumes a deficit of C in the TiC structure.

3.2. Flow curves

The compression curves are shown in Fig. 3, and for better distinction, some are slightly displaced along the x axis. All the materials show strain hardening. Unlike the other samples, unreinforced Ti grade 2 and Ti/SiC admit large compressive deformations; thus the fracture of samples was not reached. The strain hardening rates are similar for the alloys with and without reinforcement (strain hardening exponent $n \approx 3$).

In general, the addition of ceramic particles increases the flow resistance for all matrix alloys at RT but the deformation at fracture decreases significantly. The flow resistance of all samples drops significantly between RT and 350 °C.

Figure 4 shows the maximal compression stress (σ_m) and the stress at 2 % of compressive plastic deformation (σ_{p2}) of the MMC relative to the matrix at RT and 350 °C. At RT, 20 vol.% of TiC particles increase σ_{p2} of Ti662 almost by 40 %, and

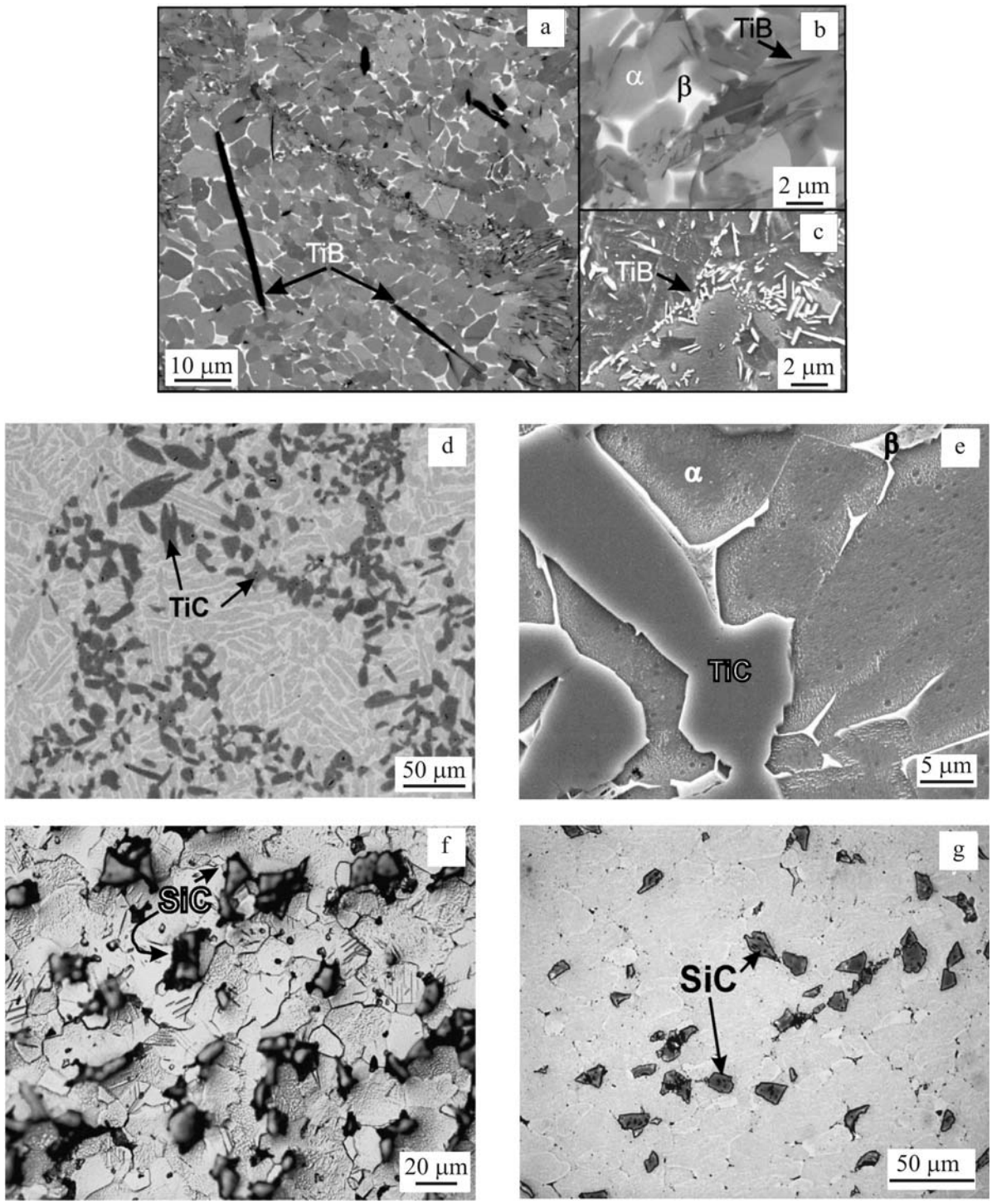

Fig. 2. Micrographs of composites: a), b), c) Ti64 reinforced with TiB showing big TiB needles and TiB whiskers (black) formed during consolidation and slow cooling; BSE and SE of an etched sample respectively showing small TiB precipitates at the alpha grain boundaries; d) Ti662 reinforced with 20–12 vol.%. TiC particles appear in black and lamellar alpha phase in dark grey; e) etched sample showing alpha and beta phases, as well as TiC particles; f), g) titanium grade 2 matrix composites reinforced with 15 vol.% and 10 vol.% of particles SiC (in black) consolidated by hot extrusion and sintering, respectively.

σ_m more than 15 % and only 5 vol.% of TiB, the σ_{p2} by more than 25 % and σ_m by around 10 %. At 350 °C, the effect of TiC and TiB particles decreases considerably. SiC increases σ_{p2} of pure Ti by more than 120 % and σ_m by more than 40 % at 350 °C.

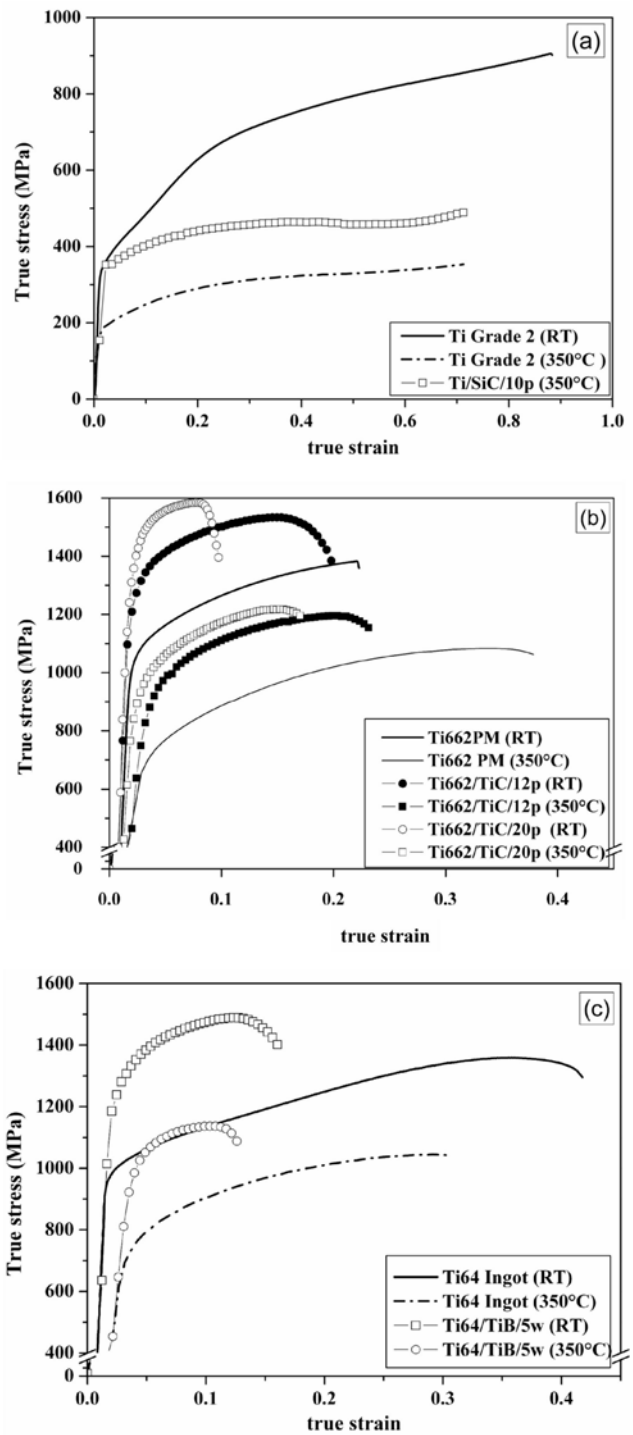

Fig. 3. Compression curves at RT and at 350 °C of a) unreinforced Ti and SiC reinforced Ti, b) unreinforced Ti64 ingot and Ti64 PM reinforced with TiB whiskers and c) unreinforced Ti662 PM and reinforced with 12 and 20 vol.% TiC particles.

3.3. Hardness

The macro- and microhardness results are shown in Fig. 5 for the MMCs and matrix alloys. The particles increase the macrohardness up to 20 % for 20 vol.% of TiC, around 14 % for 5 vol.% of TiB whiskers, and around 95 % for 15 vol.% of SiC particles in Ti. The microhardness values show no hardening of the Ti662 matrix by the addition of TiC particles, but significant hardening of Ti of around 50 % when reinforced

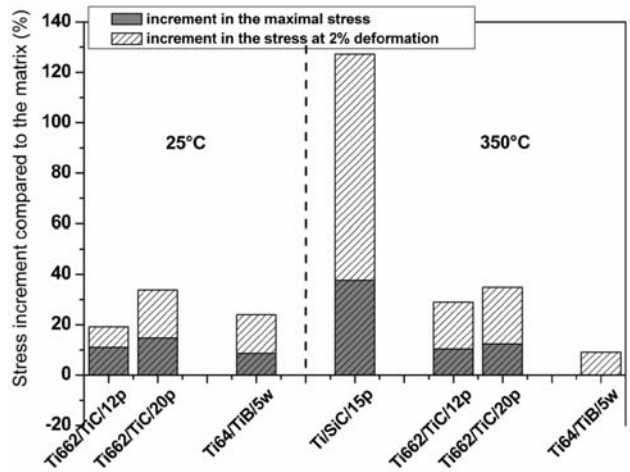

Fig. 4. Flow stress values of the composites compared to the matrix at RT and at 350 °C.

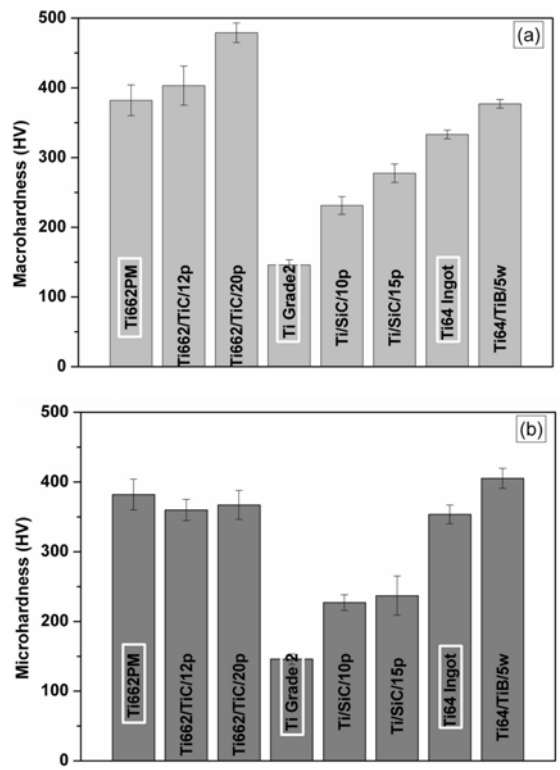

Fig. 5. Macro- and microhardness (matrix) results for the unreinforced Ti662 PM and ingot, Ti64 ingot and Ti grade 2, and their reinforced variations.

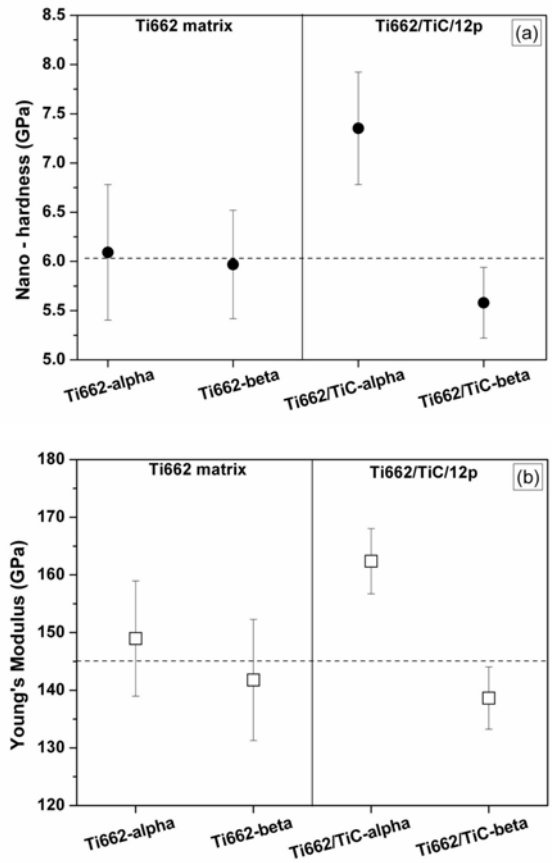

Fig. 6. Nanohardness results of Ti662 reinforced with TiC particles, showing a harder alpha phase in the reinforced material compared to the alpha of the unreinforced one.

with 10–15 vol.% SiC particles, and more than 15 % for Ti64 reinforced with 5 vol.% of TiB whiskers. In the latter case, the matrix also contains small TiB precipitates.

The nanohardness values are shown in Fig. 6a, for both alpha and beta phases of the unreinforced Ti662 and the 12 vol.% TiC reinforced alloy. The nanoindentations were done in the matrix near the TiC particles. A reinforcement effect of about 25 % can be observed in the alpha phase in the composite.

3.4. Young's modulus

The Young's moduli for different materials are shown in Fig. 7 as a function of temperature. The differences in the matrices can be related to the alloying elements (higher content of V and Sn in Ti662 than in Ti64, higher oxygen content in the powder metallurgy materials), which increase the Young's modulus [23]. All the composites present higher values of Young's modulus than their matrices, but the temperature dependence remains the same: –57 MPa K^{-1} for Ti64, and –39 MPa K^{-1} for Ti662.

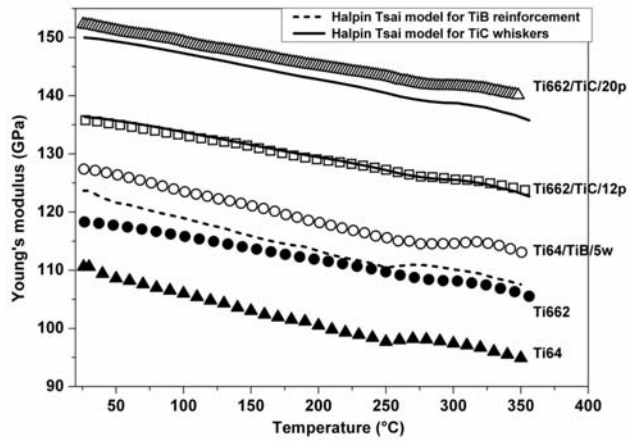

Fig. 7. Young's modulus as a function of the temperature. TiB reinforcement results in the largest increment of Young's modulus per % of reinforcement. Results of Halpin and Tsai models are also plotted.

The experimental results are compared to the Halpin Tsai model, using the measured PM-matrices' moduli. Equation (1) was applied for the materials reinforced with TiC or SiC particles. The Young's modulus of Ti64 reinforced with the TiB needles was calculated according to Eqs. (2) and (3). For all the calculations, a value of $\xi = 1$ was used, and for the TiB needles, a shape factor $S = l/d$ of 10 (from metallography) was assumed.

The model correlates very well with the results of the materials reinforced with TiC particles, although the Ti662 reinforced with 20 vol.% of particles presents higher experimental values of Young's modulus. This could be related to the clusters of TiC particles (see Fig. 2d), which can modify the "effective" aspect ratio, or to higher interstitial C concentration in the matrix compared to unreinforced Ti662. The Young's modulus obtained from the nanohardness indentation at RT shown in Fig. 6b increases in the alpha phase of Ti662/TiC about 10 %, probably due to the presence of interstitial C. The high values are due to a systematic error in the measurements.

The experimental value of Young's modulus of Ti64/TiB/5w reaches 128 GPa at RT and 113 GPa at 350 ℃. The predicted Halpin Tsai value yields 3–5 % smaller values, which is remarkable. The Young's modulus predicted by Gorsse et al. [20] is around 120 GPa for 5 vol.% of TiB, about 6 % below the experimental value at RT obtained in this work. This difference can be attributed to the 0.1 wt.% of interstitial C added to the composite during its production.

4. Discussion

SiC is the reinforcement that strengthens the

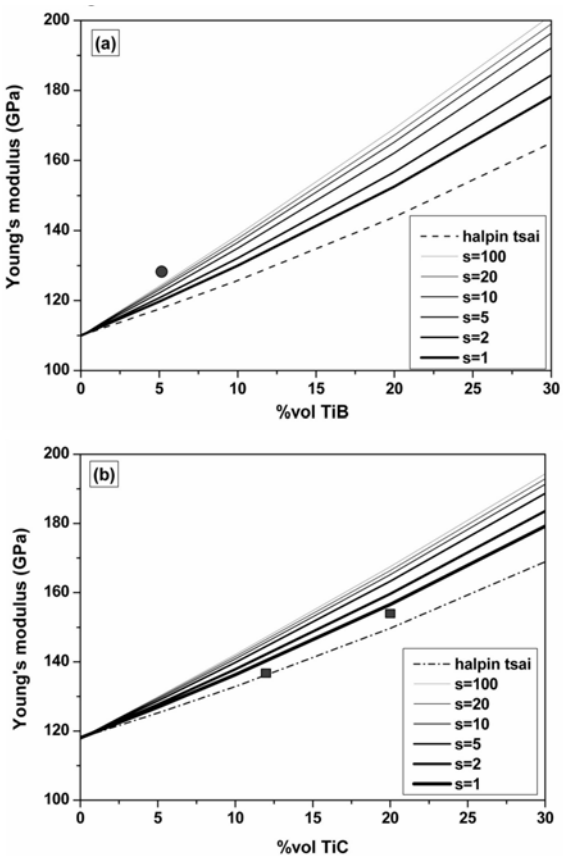

Fig. 8. Young's modulus as a function of the vol.% of particles for different geometric relations. The figures represent the measured data.

matrices significantly, even at 350 °C. The main composite strengthening mechanism is the generation of misfit strains, which are highest for SiC particles compared with TiC or TiB particles. The volume misfit $3\Delta\alpha\Delta T$ (and the estimated elastic stress, $\sigma = E_{\text{matrix}}\varepsilon$) for $\Delta T = 500$ K (above there is enhanced diffusion) are 0.7 vol.% for SiC (268 MPa), 0.2 vol.% for TiC (73 MPa) and only 0.03 vol.% for TiB (10 MPa) reinforcement.

The dislocation strengthening generated by the misfit in the coefficient of thermal expansion (α) between the matrix and the particles can be compared according to Eqs. (4) and (5), and using $b = 0.3$ nm [24] and $d = 10$ μm, $G = 40$ GPa for Ti and $G = 45$ GPa for Ti662: $\Delta\sigma_{\text{YM(SiC/15p)}} = 14$ MPa and $\Delta\sigma_{\text{YM(TiC/20p)}} = 10$ MPa.

It means that the dislocation strengthening of titanium reinforced with 15 vol.% SiC or 20 vol.% TiC particles should result in an increment in yield strength of only 1 %.

In the case of the SiC reinforced Ti, the grains are 60 μm for unreinforced Ti grade 2, and around 20 μm for the hot extruded samples, and a Hall-Petch effect can be estimated up to 1.7 times for the finer grains. An increase of 50 % in maximum flow stress and microhardness was observed in the Ti/SiC/15p sample. The microhardness values of the matrices are of the same level as the macrohardness of the composites.

In the Ti662 matrix composite, there are percolating regions of almost 40 vol.% of particles in between particle free matrix. The irregular particle distribution in the Ti662/TiC composites does not produce any strain hardening of the matrix in the particle free regions. The strengthening and the increment of the Young's modulus above the Halpin Tsai model can be attributed to the presence of interstitial C in the matrix evidenced in the nanohardness results. The increment in the lattice parameters of alpha and beta phases compared to the unreinforced material, and the smaller lattice parameter of the TiC phase compared to the literature also should be a result of interstitial C from the TiC particle.

The increase in yield strength by 5 vol.% of TiB is about 25 % at room temperature, whereas the increase in the matrix microhardness is only about 15 %. The application of the Halpin Tsai model yields a Young's modulus value close to the experimental result only when inserting an S value of 100, whereas the measured S is 10 (Fig. 8). Interstitial C coming from the original powders (0.1 wt.%) can be the cause for the high Young's modulus and can add some strengthening effect. TiB precipitates produce two important effects in the matrix, and the strengthening is the consequence of:

1. Grain refinement: The alpha phase is about 20 μm for the Ti64 ingot and 5 μm for the Ti64/TiB. It is possible to compare the contribution of the grain refinement for the matrix and for the composite by using Eq. (6): $\Delta\sigma_{\text{YM(Ti64)}} \approx 20$ MPa, $\Delta\sigma_{\text{YM(Ti64/TiB)}} = 40$ MPa. The contribution of the finer grains is twice of that of the base alloy.

2. Dispersion strengthening: TiB precipitates smaller than 100 nm formed *in situ* during the CHIPing shown in Fig. 2c, strengthen the matrix by Orowan mechanism.

5. Conclusions

1. The elastic modulus of titanium can be increased by discontinuous reinforcement:

a) +1.5 % per vol.% TiC in Ti662. The Young's modulus values for TiC reinforced titanium were correlated with the Halpin Tsai model.

b) 16 %, i.e. +3 % per vol.% TiB in Ti64, giving values above the Halpin Tsai model.

2. The temperature dependence of the Young's moduli of composites follows that of their matrices.

3. Strengthening by SiC is more effective than that by TiB and TiC due to the significant α misfit between matrix and particles, i.e. +1 to 3 % per vol.% SiC.

4. The grain refinement produced by the TiB needles results in an increment of the strength due to Hall Petch mechanisms. Furthermore, the fine TiB precipitates produce dispersion strengthening and the large TiB needles contribute like short fibre reinforcement.

Acknowledgements

The authors would like to thank Volkan Liedtke (ARCS) for the hot pressing of Ti/SiC/10p, and C. Edtmaier for the hot extruded samples (TU Vienna), the University Service Centre for Transmission Electron Microscopy, Vienna University of Technology, Austria for the FEG-SEM device. Finally we thank Prof H. P. Degischer from the Institute of Mat. Science and Technology, TU Vienna for the supervision and the revision of the manuscript.

References

[1] ZUOCHEN, L.—GUOZHEN, D. Ju.: In: Proceedings of the Int. Conf. on Products and Appl. of Titanium. Boulder, CO, Titanium Development Association 1994, p. 45.

[2] ALMAN, D. E.—HAWK, J. A.: Wear, *225*, 1999, p. 629. doi:10.1016/S0043-1648(99)00065-4

[3] LU, W. J.—ZHANG, D.—ZHANG, X. N.—WU, R. J.—SAKATA, T.—MORI, H.: Mater. Sci. Eng. A, *311*, 2001, p. 142. doi:10.1016/S0921-5093(01)00910-8

[4] POLETTI, C.—DEGISCHER, H. P.—KREMMER, S.—MARKETZ, W.: Mater. Sci. Eng. A, *486*, 2008, p. 127. doi:10.1016/j.msea.2007.08.077

[5] WAGONER JOHNSON, A. J.—KUMAR, K. S.—BRIANT, C. L.: Metall. Mater. Trans. A, *34*, 2003, p. 1869. doi:10.1007/s11661-003-0152-7

[6] SELAMAT, M. S.—WATSON, L. M.—BAKER, T. N.: J. Mater. Proc. Technol., *142*, 2003, p. 725. doi:10.1016/S0924-0136(03)00814-8

[7] POLETTI, C.—BALOG, M.—SCHUBERT, T.—LIEDTKE, V.—EDTMAIER, C. : Compos. Sci. Technol., *68*, 2008, p. 2171. doi:10.1016/j.compscitech.2008.03.018

[8] CUI, Z. D.—ZHU, S. L.—MAN, H. C.—YANG, X. J.: Surf. Coat. Technol., *190*, 2005, p. 309. doi:10.1016/j.surfcoat.2004.02.012

[9] FURUTA, T.—YAMAGUCHI, T.—SHIBATA, Y.—SAITO, T.: In: Titanium '99. III. Eds.: Gorynin, I. V., Ushkov, S. S. St. Petersburg, CRISM Prometey 2000, p. 1917.

[10] GODFREY, T. M. T.—GOODWIN, P. S.—WARD-CLOSE, C. M.: In: Titanium '99. III. Eds.: Gorynin, I. V., Ushkov, S. S. St. Petersburg, CRISM Prometey 2000, p. 1868.

[11] LAPIN, J.—ONDRUS, L.—BAJANA, O.: Mater. Sci. Eng. A, *360*, 2003, p. 85. doi:10.1016/S0921-5093(03)00445-3

[12] JOSHI, P. B.—MARATHE, G. R.—MURTI, N. S. S.—KAUSHIK, V. K.—RAMAKRISHNAN, P.: Mat. Lett., *56*, 2002, p. 322.

[13] KE GENG—WEIJIE LU—ZHIFENG YANG—DI ZHANG: Mat. Lett., *57*, 2003, p. 4054. doi:10.1016/S0167-577X(03)00264-7

[14] CLYNE, T. W.—FLOWER, H. M.: In: Titanium '92: Sci. Tech. Proceedings. Ed.: Froes, F. H. Warrendale, PA, USA, TMS 1993, p. 2467.

[15] HALPIN, J. C.—TSAI, S. W.: Environmental Factors in Composite Design. Air Force Materials Laboratory, AFML-TR-67-423.

[16] MILLER, W. S.—HUMPHREYS, F. J.: Scr. Metall. Mater., *25*, 1998, p. 33. doi:10.1016/0956-716X(91)90349-6

[17] GORSSE, S.—LE PETITCORPS, Y.: Comp. Part. A, *29*(*A*), 1998, p. 1221.

[18] FENG, H.—MENG, Q.—ZHOU, Y.—JIA, D.: Mater. Sci. Eng. A, *397*, 2005, p. 92. doi:10.1016/j.msea.2005.02.003

[19] WANJARA, P.—DREW, R. A. L.—ROOT, J.—YUE, S.: Acta Mater., *48*, 2000, p. 1443. doi:10.1016/S1359-6454(99)00453-X

[20] GORSSE, S.—LE PETITCORPS, Y.—MATAR, S.—REBILLAT, F.: Mater. Sci. Eng. A, *80*, 2003, p. 340.

[21] CHRYSANTHOU, A.—CHEN, Y. K.—VIJAYAN, A.—O'SULLIVAN, J.: J. Mater. Sci., *38*, 2003, p. 2073. doi:10.1023/A:1023562126927

[22] CRUZ FERNANDES, J.—ANJINHO, C.—AMARAL, P. M.—ROSA, L. G.—RODRIGUEZ, J.—MARTINEZ, D.—OLIVEIRA, F. A. C.—SHOHOJI, N.: Mater. Chem. Phys., *77*, 2003, p. 711. doi:10.1016/S0254-0584(02)00131-1

[23] CONRAD, H.: Progr. Mat. Sci., *26*, 1981, p. 123. doi:10.1016/0079-6425(81)90001-3

[24] SURI, S.—VISWANATHAN, G. B.—NEERAJ, T.—HOUL, D.-H.—MILLS, M. J.: Acta Mater., *47*, 1999, p. 1019. doi:10.1016/S1359-6454(98)00364-4